7. T. Webb III *et al.*, in *North America and Adjacent Oceans During the Last Glaciation*, W. F. Ruddiman and H. E. Wright, Jr., Eds. (Geological Society of America, Boulder, CO, 1987), pp. 447–462; T. Webb III, *Vegetatio* **69**, 177 (1987).
8. I. C. Prentice, in *Vegetation History*, B. Huntley and T. Webb III, Eds. (Kluwer Academic, Dordrecht, the Netherlands, 1988), pp. 17–42.
9. The split of pines into northern and southern groups was based on the contemporary range maps in E. L. Little, *Atlas of United States Trees,* vol. 1 of *Conifers and Important Hardwoods* (U.S. Department of Agriculture, Washington, DC, 1971). A pollen sum of all tree, shrub, and herb pollen was used to calculate pollen percentages.
10. P. J. Bartlein, I. C. Prentice, T. Webb III, *J. Biogeogr.* **13**, 35 (1986); I. C. Prentice and A. M. Solomon, in *Global Changes of the Past*, R. S. Bradley, Ed. (Office for Interdisciplinary Earth Studies, University Corporation for Atmospheric Research, Boulder, CO, 1991), pp. 365–383; see also (7). The latest generation of static models also includes the physiologically based IIASA Biome Model (A. M. Solomon, personal communication).
11. We fit the response surfaces using a three-step procedure: (i) a rectangular grid was generated in the climate space defined by mean January temperature, July temperature, and annual precipitation; (ii) at each grid point, the locally weighted average abundance of a particular pollen type was calculated; and (iii) the surface was depicted by interpolating among those values. Further details may be found in B. Huntley, P. J. Bartlein, I. C. Prentice [*J. Biogeogr.* **16**, 551 (1989)].
12. Output from three different GCMs was used as equilibrium climate for doubled CO_2 levels for eastern North America: (i) the NASA GISS Model II 7.8° latitude by 10.0° longitude GCM [Hansen *et al.*, *Mon. Weather Rev.* **111**, 609 (1983); Hansen *et al.*, in *Climate Processes and Climate Sensitivity*, J. E. Hansen and T. Takahashi, Eds. (American Geophysical Union, Washington, DC, 1984), pp. 130–163]; (ii) the GFDL 4.4° by 7.5° GCM [S. Manabe and R. T. Wetherald, *J. Atmos. Sci.* **44**, 1211 (1987)]; and (iii) the OSU 4.0° by 5.0° GCM [M. Schlesinger and Z. Zhao, "Seasonal climate changes induced by doubled CO_2 as simulated by the OSU atmospheric GCM/mixed layer ocean model" (Oregon State University, Climate Research Institute, 1988)]. Because these models have different sensitivities and regional responses, they provide a useful range of possible future climate scenarios. More detailed descriptions of the scenarios for the three GCMs used are given in J. B. Smith and D. Tirpak, "The potential effects of global climate change on the United States" (Rep. EPA-230-05-89-50, U.S. Environmental Protection Agency, Washington, DC, 1989).
13. Modern (0 ka) control GCM experiments all exhibit systematic biases when compared to observed modern climate (*2, 7*). In order to minimize the potential effects of these biases in our analyses, we applied simulated climate anomalies (experiment with doubled CO_2 levels minus control experiment) to observed modern climate normals (1951 to 1980) for the region.
14. J. T. Overpeck and P. J. Bartlein, in *Rep. EPA-230-05-89-50* (U.S. Environmental Protection Agency, Washington, DC, 1989), chap. 1.
15. To construct the maps of observed pollen data, we used pollen data from 860 samples collected from the surficial (modern) sediments of lakes and mires across eastern North America (*14*) and interpolated these onto a 100-km equal-area grid. The mapped patterns in the observed pollen data reflect the regional vegetation patterns, relatively undisturbed by the effects of settlement by Europeans (*19*).
16. We produced these maps by interpolating the fossil data in (7).
17. We first used linear interpolation to assign pollen spectra at each of 243 radiocarbon-dated pollen records (*14*) to time series with a 250-year sampling interval. We then used an inverse-distance weighting method (7) to interpolate fossil pollen data for the seven pollen types (Fig. 1) to the same 100-km equal-area grid that was used to interpolate the doubled CO_2 simulations (*13*) and present observed pollen (*15*). We calculated the squared chord distances (d_{ij}) between pairs of pollen spectra (i and j) using:

$$d_{ij} = \Sigma_k (p_{ik}^{1/2} - p_{jk}^{1/2})^2$$

Where p_{ik} is the proportion of pollen type k in pollen spectrum i. The theoretical and empirical advantages of using this dissimilarity coefficient with pollen data are discussed in (*18*).
18. J. T. Overpeck *et al.*, *Quat. Res.* **23**, 87 (1985).
19. G. L. Jacobson, T. Webb III, E. C. Grimm, in *North America and Adjacent Oceans During the Last Glaciation*, W. F. Ruddiman and H. E. Wright, Jr., Eds. (Geological Society of America, Boulder, CO, 1987), pp. 277–288.
20. T. Webb III, in *Vegetation History*, B. Huntley and T. Webb III, Eds. (Kluwer Academic, Dordrecht, the Netherlands, 1988), pp. 385–414.
21. R. D. Cess *et al.*, *Science* **245**, 513 (1989).
22. A. M. Solomon, *Oecologia* **68**, 567 (1986); D. B. Botkin *et al.*, in *Rep. EPA-230-05-89-50* (U.S. Environmental Protection Agency, Washington, DC, 1989), chap. 2.
23. J. T. Overpeck, D. Rind, R. Goldberg, *Nature* **343**, 51 (1990).
24. C. Zabinski and M. B. Davis, in *Rep. EPA-230-05-89-50* (U.S. Environmental Protection Agency, Washington, DC, 1989), chap. 5; W. Emanuel, H. Shugart, M. Stevenson, *Clim. Change* **7**, 457 (1985); D. Lashof, thesis, University of California, Berkeley (1987); K. C. Prentice and I. Y. Fung, *Nature* **346**, 48 (1990).
25. M. B. Davis, *Ann. Mo. Bot. Gard.* **70**, 550 (1983).
26. B. Huntley and T. Webb III, Eds., *Vegetation History* (Kluwer Academic, Dordrecht, the Netherlands, 1988).
27. A. J. Gear and B. Huntley, *Science* **251**, 544 (1991).
28. A. M. Solomon and D. C. West, in *Rep. DOE/ER-0236* (U.S. Department of Energy, Washington, DC, 1985), pp. 145–169; J. Pastor and W. M. Post, *Nature* **334**, 55 (1988).
29. B. R. Strain, *Biogeochemistry* **1**, 219 (1985).
30. This research was supported by a grant from the U.S. Environmental Protection Agency under Interagency Agreement number DW80932629-01 and by the National Science Foundation Climate Dynamics Program. The support of facilities and colleagues at the National Aeronautics and Space Administration Goddard Institute for Space Studies is gratefully acknowledged. We thank R. Goldberg for technical assistance and B. Lipsitz for help with graphics. A. Solomon, J. Cole, E. Cook, L. Donet, G. Jacoby, M. Kneller, and R. Webb provided valuable reviews and discussions of the manuscript. This is Lamont-Doherty Geological Observatory Contribution no. 4838.

11 April 1991; accepted 26 July 1991

Synorogenic Collapse: A Perspective from the Middle Crust, the Proterozoic Grenville Orogen

K. MEZGER, B. A. VAN DER PLUIJM, E. J. ESSENE, A. N. HALLIDAY

Structural, petrological, and geochronological studies of the middle to late Proterozoic Grenville orogen in Ontario, Canada, indicate that a major extensional fault developed synchronously with late thrusting. This fault zone was initiated during peak metamorphism and extended into the crust to depths of at least 25 kilometers. The temporal and spatial relations among faulting, metamorphism, and regional compression indicate that synorogenic collapse initiated because the crust exceeded the maximum physiographic height and thickness that could be supported by its rheology. Comparison of Grenville with recent Himalayan orogenic activity suggests that during Proterozoic times physiographic height, crustal thickness, and crustal strength were similar to modern conditions in orogenic belts.

THE DEVELOPMENT OF LARGE-SCALE extensional shear zones and associated rapid thinning of tectonically thickened continental crust is increasingly recognized as a major synorogenic to postorogenic process referred to as "orogenic collapse." Theoretical arguments have been advanced that require extensional tectonics as a consequence of crustal thickening due to compressional tectonics (*1, 2*). Many orogenic belts develop extensional shear zones after the compressional forces cease (*1, 3–5*). Only in a few cases has it been shown that extensional shear zones develop in the upper parts of active orogenic belts while the crust is still undergoing compression (*1, 2*). In this report we provide evidence from the Proterozoic Grenville orogen that synorogenic collapse due to crustal overthickening occurred also in ancient orogenic belts and that collapse structures extended into the middle crust.

The Grenville orogen extends from Labrador to central Mexico and continues on the eastern side of the Atlantic Ocean in Ireland and Scandinavia (*6, 7*). Thus, in extent the Grenville orogen is comparable to the Cordillera of western North America and the Alpine-Himalayan mountain chain. The Grenville orogen is exposed continuously from Labrador to southern Ontario and northern New York. Elsewhere its extent is inferred from small isolated exposures, inliers within younger orogenic belts, xenoliths brought up in young volcanic rocks, drill holes, and geophysical studies [for example (*8, 9*)]. Most of the exposed Grenville orogen is made up of rocks that have experienced at least amphibolite facies metamorphism (550° to 650°C at 6 to 8 kbar), and a large part has undergone granulite facies metamorphism (700° to 800°C at 6 to 11 kbar) [for example (*10*)]. Thus, in

Department of Geological Sciences, C. C. Little Building, The University of Michigan, Ann Arbor, MI 48109.

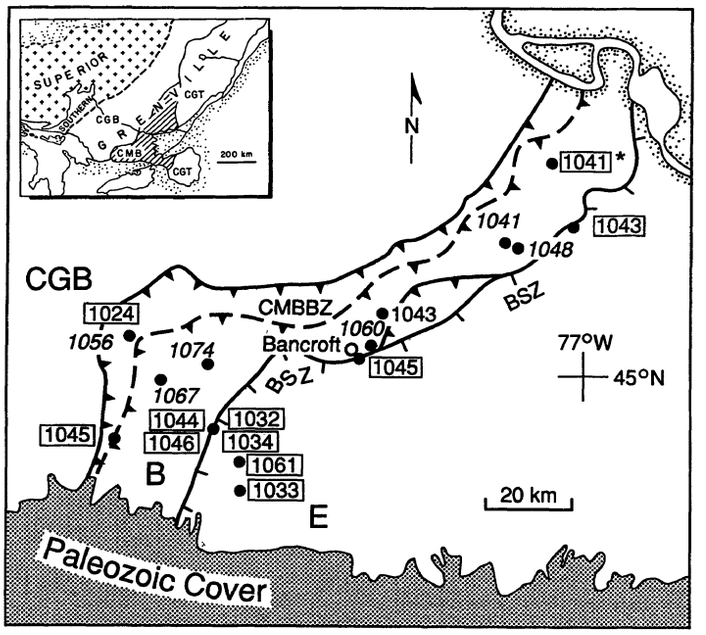

Fig. 1. Simplified geologic map of the northwestern Central Metasedimentary belt and southeastern Central Gneiss belt of Ontario. Shown are the major faults and the direction of movement as recorded by shear sense indicators within the shear zones. The numbers correspond to the U-Pb ages given in Table 1. Ages in boxes correspond to metamorphic sphenes from marbles, calc-silicate gneisses, and an amphibolite and monazite from a metapelite (marked by a "*"). The other ages correspond to sphenes that grew most likely as a result of igneous activity and were extracted from granites, syenites, pegmatites, and skarns. E, Elzevir domain; B, Bancroft domain; CMB, Central Metasedimentary belt; CMBBZ, Central Metasedimentary belt boundary zone; CGB, Central Gneiss belt; CGT, Central Granulite terrane; and BSZ, Bancroft shear zone.

contrast to young mountain belts such as the Alpine-Himalayan chain, the Grenville orogen allows a direct view of processes that were active in the middle to lower crust during orogenic activity.

The southern part of the exposed Grenville orogen can be subdivided on the basis of distinctive associations of lithologies, geophysical data, and metamorphic histories into three large belts that strike approximately parallel to the orogen. From northwest to southeast, these are the Central Gneiss belt, the Central Metasedimentary belt, and the Central Granulite terrane (Fig. 1) (*11*). The first two belts are bounded to the northwest by ductile thrust zones: the Grenville Front tectonic zone and the Central Metasedimentary belt boundary zone (CMBBZ), respectively (*11–13*) (Fig. 1). The Central Gneiss belt is dominated by metaigneous gneisses that were metamorphosed in the upper amphibolite or granulite facies and consists of several domains that are bounded by northwest-directed thrust faults (*12–14*). The Central Metasedimentary belt has been subdivided into several domains, of which two, the Bancroft and Elzevir domains, are shown in Fig. 1. The domains are separated from each other by ductile shear zones. However, the direction of movement along these shear zones is largely unknown except for the Bancroft shear zone, which runs approximately parallel and in some places crosscuts the boundary between the Bancroft and the Elzevir domains (Fig. 1). This shear zone is a southeast-dipping fault zone in which all structures (including rotated clasts, S-C structures, shear bands, and mica fish) indicate a normal sense of motion (*15*). In addition, a discontinuity in metamorphic grade is observed across this fault. In the vicinity of Bancroft (Fig. 1) the rocks are of upper amphibolite facies, whereas the immediately adjacent parts of the Elzevir domain are of only middle amphibolite facies (*15–17*). Graphite-calcite carbon isotope thermometry on mylonitized marbles indicates that the shear zone was active down to temperatures of about 500°C (*18*).

In order to evaluate the geological importance of this extensional fault it is essential to determine the time of shearing with respect to regional thrusting and peak metamorphism. Therefore, U-Pb ages were obtained for metamorphic sphenes from marbles and calc-silicate gneisses within and from either side of the shear zone. In addition, sphenes were selected from skarns and igneous intrusions in order to evaluate the timing and significance of magmatism with respect to metamorphism and tectonism.

Sphene was chosen because it is the only widespread mineral suitable for isotopic dating that is of unambiguously metamorphic origin in marbles and calc-silicate gneisses. In addition, sphene is the only widespread and abundant metamorphic mineral that can be used to obtain precise growth ages in the Central Metasedimentary belt [Table 1 (*19*)]. Sphene has an apparent closure temperature for the U-Pb system of about 550° to 650°C, depending on the grain size (*20*). Because the highest metamorphic temperatures in this area were 600°C, and 650°C may have been reached only locally (*14*), it is possible to obtain information on the timing of prograde metamorphism as well as its duration from analyses of sphenes. Mylonitization continued down to about 500°C (*18*), and therefore newly grown sphenes within the shear zone can be used to determine directly the time of shearing and recrystallization in the Bancroft shear zone.

The U-Pb ages obtained on metamorphic sphenes from samples within and outside the Bancroft shear zone range from 1045 to 1030 Ma (million years ago), (Fig. 1 and Table 1). In contrast, sphenes that grew as a result of igneous activity are older than 1041 Ma. Because the igneous sphenes were not reset isotopically by the metamorphism, the ages of the metamorphic sphenes are interpreted as growth ages. In addition a monazite from a metapelite was dated at 1041 ± 2 Ma. Because monazite has a closure temperature for the U-Pb system of about 725° ± 25°C (*21*), this age corresponds to the time of mineral growth and dates the regional metamorphism.

Morphology, color, and inclusion pattern of sphenes from sheared marbles are distinct from sphenes that were extracted from unsheared samples. However, there is no systematic variation in the U-Pb ages among these sphenes. To illustrate this relation further, sphenes from a hand specimen that consists of unsheared and mylonitized parts (samples 90-45, Table 1) were examined in detail. The unsheared marble contains coarse calcite and graphite together with

Table 1. U-Pb sphene ages in millions of years ago. Gr, granite; Sy, syenite; CSG, calc-silicate gneiss; Peg, pegmatite; MM, marble mylonite; Sk, skarn; M, marble; Pel, pelite; Am, amphibolite. Errors are ±2 SEM.

Sample	$^{206}Pb/^{238}U$	$^{207}Pb/^{235}U$	$^{207}Pb/^{206}Pb$	Rock type
90-38	1074	1074	1074 ± 2	Gr
90-39	1068	1068	1067 ± 2	Sy
89-05	1058	1059	1060 ± 3	Sy
90-46	1057	1059	1061 ± 2	CSG
90-88b	1053	1054	1056 ± 3	Gr
ACP/3	1049	1049	1048 ± 2	Peg
5D	1041	1043	1046 ± 1	MM
BA-28	1044	1044	1045 ± 2	MM
90-40	1045	1045	1045 ± 2	CSG
89-06/1	1044	1043	1043 ± 2	Sk
89-06/2	1041	1042	1044 ± 4	Sk
GO4b	1047	1046	1044 ± 1	MM
89-18/1	1015	1024	1042 ± 4	M
89-18/2	1043	1043	1043 ± 6	M
ZR.15	1042	1042	1041 ± 3	Peg
REN-28*	1042	1042	1041 ± 2	Pel
90-45	1035	1035	1034 ± 3	MM
90-45	1029	1030	1032 ± 2	M
90-47	1033	1033	1033 ± 2	CSG
90-88	1025	1025	1024 ± 2	Am

*Monazite.

inclusion-free, dark brown sphenes (5 to 10 mm across) with well-developed crystal faces; the marble mylonite consists of fine-grained calcite with graphite coatings and has small (<0.5 mm), disk-shaped, yellow-brown sphenes without any crystal faces but abundant inclusions. The two sphene samples are also markedly distinct in their U and Pb concentrations and their Pb-isotope ratios. These relations imply that the sphenes from the shear zones are not rounded fragments that were once part of larger sphenes that grew before shearing but rather are newly grown grains that formed during mylonitization. Both types of sphene yielded identical concordant ages of 1032 ± 2 Ma and 1034 ± 3 Ma, respectively (Table 1). Sphenes from two other samples of strongly sheared marble from the same outcrop yielded ages of 1044 ± 1 Ma and 1046 ± 1 Ma. The total spread in concordant U-Pb sphene ages from the Bancroft shear zone (Fig. 1) is interpreted to indicate that the shear zone was active from about 1045 to 1030 Ma. The older sphene ages from sheared samples are identical to the interval of monazite and sphene growth in unsheared rocks in the vicinity of the Bancroft shear zone. From this relation we conclude that peak metamorphism coincided with the initiation of normal faulting. The temperatures of about 500°C for the mylonitized marbles indicate that shearing continued during cooling.

The initiation of thrusting of the Central Metasedimentary belt onto the Central Gneiss belt along the CMBBZ (Fig. 1) was dated with the U-Pb technique on zircons extracted from syntectonic pegmatites located within the shear zone (*22, 23*). The ages indicate that thrusting started at about 1160 Ma in the northeast parts of the CMBBZ. Major reimbrication and thrusting along the whole shear zone was initiated at 1060 Ma, about 20 million years before peak metamorphism at about 1040 Ma. Thrusting lasted until at least 1025 Ma, as is indicated by U-Pb zircon ages from the northeastern part of the CMBBZ (*22, 23*) and the growth of the last metamorphic sphenes in parts of the CMBBZ (sample 90-88, Table 1, and Fig. 1). The whole Grenville orogen of Ontario and northern New York continued to undergo compression at least until about 1000 Ma (*16, 24*). Because extension along the Bancroft shear zone coincided with thrusting in immediately adjacent parts and throughout the orogen, this shear zone is interpreted to be a synorogenic collapse structure.

Stable continental crust is approximately 35 km thick and has an elevation that is typically only a few hundred meters above sea level. In contrast, collisional tectonics in active orogenic belts, which leads to thrusting and crustal shortening, may produce continental crust with at least twice its normal thickness and a maximum average physiographic height of 5 km (*1, 25*). Since the crust reaches isostatic equilibrium on a timescale of 10^4 years (*26*), the resulting mountain range reaches its maximum physiographic height at about the same time the crust reaches its maximum thickness. The maximum thickness and physiographic height of the crust are constrained by its strength and the magnitude of the lateral compressional forces. Once the crust reaches a physiographic height that cannot be supported further by the strength of the rock column, the rocks in the lower part of the crust may flow laterally or extensional shear zones may develop in the upper parts of the thickest crust. Evidence for crustal thinning due to lateral flow is not accessible to direct observation. However, evidence of orogenic collapse is preserved as prominent normal faults that parallel orogenic belts [for example (*2*)]. During synorogenic collapse, normal faulting leads to crustal thinning by extension of crustal segments in an area that is undergoing compression on a regional scale. The topographic expression of the mountain range will be balanced by extension during continued crustal shortening. Such a scenario is consistent with the observations in the northern Central Metasedimentary belt.

The Central Metasedimentary belt was emplaced on the Central Gneiss belt, which was thickened previously by thrusting from 1160 to 1120 Ma (*13*). The second episode of thrusting along the CMBBZ that started at 1060 Ma led to the formation of overthickened crust and a topographic front. This resulted in overstepping of the critical crustal thickness and led to the formation of an extensional shear zone parallel to the orogenic belt; this shear zone prevented further crustal thickening in the western Central Metasedimentary belt. Sphenes from igneous rocks and skarns within the Bancroft domain yielded U-Pb ages that range from 1041 to 1074 Ma and are significantly older than metamorphic sphenes (Table 1). This difference implies that most of the magmatic activity preceded peak metamorphism, and is an indication that the heat budget for metamorphism was not strongly influenced by magmatism, but rather that metamorphism was the result of crustal thickening. This lack of external heat input accounts for the low average geothermal gradient of 20° to 23°C per kilometer derived for peak metamorphism in the Central Gneiss belt and the western Central Metasedimentary belt (*14*). Such a gradient indicates that thermally undisturbed continental crust was stacked during thrusting. The U-Pb sphene data show that initial failure of the crust occurred at the time of peak metamorphism at about 1040 Ma. Uplift associated with extension led to cooling of the rocks in the footwall and halted amphibolite facies metamorphism. As a consequence no new metamorphic sphenes formed in the rocks after 1032 Ma (Fig. 1).

The observed coincidence of peak metamorphism and the initiation of orogenic collapse in the western Central Metasedimentary belt is consistent with temperature-controlled crustal weakening. This observation suggests that crustal thickness in orogenic belts is limited by the strength of the rock column and not lateral compressional forces. During peak metamorphism maximum pressures of 7 to 8 kbar (*14*) were reached in the northwestern Central Metasedimentary belt. For an average crustal density of 2.75 g/cm^3, these pressures correspond to a burial depth of 26 to 29 km. If the area was underlain by the same crust as it is now, the crust reached a maximum thickness of at least 60 to 65 km during the Grenville orogeny.

The setting of the Grenville orogen is strikingly similar to that described for the present-day central Himalayan and southern Tibetan regions, where a compressional orogenic belt shows evidence for synorogenic extension (*2*). In this young orogenic belt, southward thrusting of the Tibetan Plateau over the Indian plate has led to the formation of continental crust up to 70 km thick and an average physiographic height of 5 km (*1, 25*). This overthickened crust has collapsed along major faults that have developed parallel to the orogenic belt and terminate at unspecified levels in the continental crust (*2*). The similarity of synorogenic extension in the Grenville orogen with that described from the Himalayas (*2*) and possibly the Andes (*1*) indicates that the maximum thickness of continental crust and the possible physiographic height of mountain ranges in the Proterozoic were quite similar to the maximum values observed in currently active fold-and-thrust belts, and no differences in lower crustal viscosity or the magnitude of lateral tectonic forces have to be postulated. Moreover, the evidence for synorogenic collapse in the Grenville orogen demonstrates that extensional faults can extend at least into the middle crust (>25 km depth) and that they are initiated during peak metamorphism.

REFERENCES AND NOTES

1. J. F. Dewey, *Tectonics* 7, 1123 (1988).
2. B. C. Burchfiel and L. H. Royden, *Geology* **13**, 679 (1985).
3. J. P. Platt, *Geol. Soc. Am. Bull.* 97, 1037 (1986).

4. T. B. Anderson and B. Jamtveit, *Tectonics* **9**, 1097 (1990).
5. T. R. Charlton, *Geology* **19**, 29 (1991).
6. A. J. Baer, in *Precambrian Plate Tectonics*, A. Kröner, Ed. (*Dev. Precambrian Geol. 4*, Elsevier, Amsterdam, 1981), pp. 353–385.
7. R. H. Verschure, in *The Deep Proterozoic Crust in the North Atlantic Provinces*, A. C. Tobi and J. L. R. Touret, Eds. (NATO ISI Ser. C158, Reidel, Dordrecht, 1985), pp. 381–410.
8. M. J. Bartholomew, E. R. Force, A. Krishna Sinha, N. Herz, Eds., *Geol. Soc. Am. Spec. Pap. 194* (1984).
9. P. J. Patchett and J. Ruiz, *Contrib. Mineral. Petrol.* **96**, 523 (1987).
10. J. A. Fraser, W. W. Heywood, M. A. Mazurski, *Geol. Surv. Can. Map 1475A* (1978).
11. H. R. Wynne-Edwards, *Geol. Assoc. Can. Spec. Pap.* **11**, 263 (1972).
12. A. Davidson, in *Precambrian Tectonics Illustrated*, A. Kröner and R. Greiling, Eds. (Elsevier, Amsterdam, 1984), pp. 263–279.
13. ———, *Geol. Assoc. Can. Spec. Pap.* **31**, 61 (1986).
14. L. M. Anovitz and E. J. Essene, *J. Petrol.* **31**, 197 (1990).
15. K. A. Carlson, B. A. van der Pluijm, S. Hanmer, *Geol. Soc. Am. Bull.* **102**, 174 (1990).
16. R. M. Easton, *Geol. Assoc. Can. Spec. Pap.* **31**, 127 (1986).
17. D. M. Carmichael, J. M. Moore, G. B. Skippen, in *Field Trips Guidebook, Geol. Soc. Am.–Geol. Assoc. Can.–Mineral Assoc. Can. Meeting Toronto*, A. L. Currie and W. O. Mackasey, Eds. (Geological Association of Canada, Toronto, 1978), pp. 325–346.
18. B. A. van der Pluijm and K. A. Carlson, *Geology* **17**, 161 (1989).
19. The complete data set is available from the authors upon request. Analytical procedures are described in detail in (20).
20. K. Mezger, C. M. Rawnsley, S. R. Bohlen, G. N. Hanson, *J. Geol.* **99**, 415 (1991).
21. R. R. Parrish, *Can. J. Earth Sci.* **27**, 1431 (1991).
22. O. van Breemen and S. Hanmer, *Curr. Res. Part B Geol. Surv. Can.* **86-1B**, 775 (1986).
23. S. J. McEachern, S. Hanmer, O. van Breemen, *Geol. Assoc. Can.–Mineral. Assoc. Can. Abstr. Progr.*, p. A87 (1990).
24. K. Mezger, B. A. van der Pluijm, E. J. Essene, A. N. Halliday, *Eos* **71**, 1659 (1990).
25. P. C. England and P. Molnar, *Geology* **18**, 1173 (1990).
26. L. M. Cathles, *The Viscosity of the Earth's Mantle* (Princeton Univ. Press, Princeton, NJ, 1975).
27. This work was funded by National Science Foundation grants EAR 88-05083, 89-03805, and 90-04302. We thank T. Boundy, J. T. Chesley, G. R. Davies, C. P. DeWolf, and H. N. Pollack for comments on earlier drafts of this paper. Helpful reviews were provided by A. Davidson and an anonymous reviewer. We thank R. M. Easton and A. Davidson for sharing their insights into Grenville geology.

6 May 1991; accepted 1 August 1991

Length of the Solar Cycle: An Indicator of Solar Activity Closely Associated with Climate

E. FRIIS-CHRISTENSEN AND K. LASSEN

It has recently been suggested that the solar irradiance has varied in phase with the 80- to 90-year period represented by the envelope of the 11-year sunspot cycle and that this variation is causing a significant part of the changes in the global temperature. This interpretation has been criticized for statistical reasons and because there are no observations that indicate significant changes in the solar irradiance. A set of data that supports the suggestion of a direct influence of solar activity on global climate is the variation of the solar cycle length. This record closely matches the long-term variations of the Northern Hemisphere land air temperature during the past 130 years.

MUCH SCIENTIFIC EFFORT HAS been exercised in order to understand the effects on climate of the release of increased quantities of CO_2 into the atmosphere. Because realistic experiments on a global scale are not possible, verification of physical theories have relied on model simulations or observations. Model simulations are limited by the necessary assumptions, and observations suffer from the lack of sufficiently long time series of fundamental quantities.

One of the most fundamental quantities in relation to the terrestrial climate is the sun's radiation. This is one of the parameters of which we have the least exact knowledge. Eddy (*1*) pointed out that apparent long-term relations between solar activity and certain indicators of the global climate might be caused by changes in the solar irradiance. Only recently, however, during the satellite era, have reliable measurements of the variability of the sun's irradiance been obtained (*2*), but these measurements are for a time scale shorter than a solar cycle.

Reid (*3*) discussed a striking similarity between the globally averaged sea-surface temperature (SST) and the long-term record of solar activity, as represented by the 11-year running mean Zürich sunspot number. He pointed out that although not identical, the two time series had several features in common. Most noteworthy was the prominent minimum in the early decades of this century, the steep rise to a maximum in the 1950s, a brief drop during the 1960s and early 1970s followed by a final rise, which apparently has not stopped.

Reid used these observations to show that the solar irradiance may have varied by approximately 0.6% from 1910 to 1960 in phase with the 80- to 90-year cycle (the Gleissberg period) represented by the envelope of the 11-year solar activity cycle. To estimate the response of the upper ocean to changes in the solar constant, Reid used a simple one-dimensional ocean thermal model of Hoffert *et al.* (*4*). He found that the necessary range of variation in the solar constant required to account for the temperature increase during the 130-year period is less than 1%, which is consistent with the magnitude of the long-term trend that could be derived from the measurements of the solar irradiance.

Correlations regarding sun-weather relations have traditionally been attacked for two main reasons. The first, and perhaps most serious one, is the lack of a physical mechanism that could lead to the claimed relations. The second has been the poor statistical significance of the correlations.

Kelly and Wigley (*5*) argued that the required change in the sun's energy output largely exceeds the changes that are suggested by direct measurements. On the basis of directly measured irradiance data from the short time period of satellite measurements, Foukal and Lean (*6*) constructed a model of the total solar irradiance variation between 1874 and 1988. Variations of less than 1.1 W/m^2, which is less than 0.1% of the total output, were predicted. However, they explicitly noted that additional low-frequency changes in the irradiance might be present that could not be deduced from the limited series of irradiance data.

Even for a change in the solar energy output compatible with the value estimated by Reid, model calculations by Kelly and Wigley (*5*) indicated that solar forcing is unlikely to have accounted for more than a small part of the observed temperature variation. An important reason for this conclusion was the limited statistical correlation between the two time series used by Reid.

There is, however, no a priori reason to believe that the long-term changes of solar irradiance are perfectly represented by the number of sunspots. In this paper we pre-

Danish Meteorological Institute, Lyngbyvej 100, DK-2100 Copenhagen Ø.